


 Cite this: *RSC Adv.*, 2017, 7, 51298

 Received 16th August 2017  
Accepted 27th October 2017

DOI: 10.1039/c7ra09062e

[rsc.li/rsc-advances](http://rsc.li/rsc-advances)

# Hematite nanoparticle clusters with remarkably high magnetization synthesized from water-treatment waste by one-step “sharp high-temperature dehydration”†

 L. Yu. Novoselova 

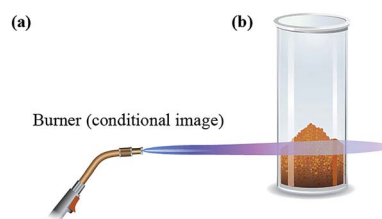
Hematite ( $\alpha$ -Fe<sub>2</sub>O<sub>3</sub>) nanoparticle clusters with an exceptionally high magnetization (51 emu g<sup>-1</sup>), comparable to that of nanoscale Fe<sub>3</sub>O<sub>4</sub> and  $\gamma$ -Fe<sub>2</sub>O<sub>3</sub>, were synthesized for the first time. This material was prepared from water-treatment waste (iron removal precipitate) after single-step exposure to high temperature without any support (template, catalyst, surfactant, or others). The key factor was the using of a new approach, namely, “sharp high-temperature dehydration” of iron hydroxides containing adsorbed water.

Nanomaterials based on iron oxides have attracted a great deal of global research interest because of their ready availability, low cost, environmental compatibility, high performance, and wide range of uses.<sup>1</sup> Iron oxide-based nanomaterials are highly promising materials that are used in diverse fields such as environmental protection and remediation,<sup>2</sup> catalysis,<sup>3</sup> sensing (e.g., of alcohols and gases such as CO, NO<sub>2</sub>, etc.),<sup>4</sup> energy storage and conversion,<sup>5</sup> biotechnology, and medicine.<sup>6</sup> Such nanomaterials have been used in the development of pigments,<sup>7</sup> electromagnetic-wave-absorbing materials,<sup>8</sup> and other products. However, syntheses of iron oxide-based nanomaterials generally include iron salts (as Fe<sup>x+</sup> precursors), nonaqueous solvents, and surfactants (which contradicts the principles of “green chemistry”); sometimes, catalysts, templates, oxidizers, fuels, and other substances are also necessary.<sup>10</sup> These processes often suffer from one or more disadvantages, including their multistage character, complexity of hardware design, duration, pollution from toxic reagents, high cost due to the use of expensive reagents, and the use of nonrenewable sources of iron.

Magnetite (Fe<sub>3</sub>O<sub>4</sub>)- and maghemite ( $\gamma$ -Fe<sub>2</sub>O<sub>3</sub>)-based nanomaterials have drawn interest primarily because of their magnetic properties,<sup>11</sup> which enable their manipulation using external magnetic fields. The magnetization values for bulk Fe<sub>3</sub>O<sub>4</sub> and bulk  $\gamma$ -Fe<sub>2</sub>O<sub>3</sub> are ~90 and ~74 emu g<sup>-1</sup>,<sup>12</sup> respectively, and as their particle sizes decrease to the nanoscale range, their magnetizations noticeably decline.<sup>13</sup> Hematite ( $\alpha$ -Fe<sub>2</sub>O<sub>3</sub>) is

conventionally considered non-magnetic iron oxide, and is not regarded as a material for applications that require external magnetic fields. According to prior reports, its magnetization value is typically less than 1 emu g<sup>-1</sup>.<sup>14</sup>

However, recent research has shown that materials may change their properties or even acquire completely new and unique properties upon nanonization.<sup>15</sup> For example, hematite nanoparticles and nanorods, recently synthesized, demonstrated a magnetization of 21, 85, and 65 emu g<sup>-1</sup>.<sup>16</sup> In these cases, a template-assisted synthesis was integrated with a high-temperature combustion stage;<sup>16a</sup> other procedures included pulse galvanostatic synthesis in the presence of external magnetic fields followed by calcination<sup>16b</sup> and microwave combustion synthesis.<sup>16c</sup> However, the reported procedures have some drawbacks, for example, a greater number of materials and reagents used (template, oxidizer, and fuel<sup>16a</sup> and nucleation starter<sup>16b</sup>) and rather cumbersome template synthesis and iron-impregnation stages.<sup>16a</sup> Also it should be noted here that in all cases, the source of Fe<sup>3+</sup> was not a renewable material<sup>16</sup> (Table S3 and Section 3.4, ESI†).



**Scheme 1** Schematic representation of the synthesis of HNPCs: (a) burner (schematic image), and (b) initial iron removal precipitate (IRP) material.

*Institute of Petroleum Chemistry, Siberian Branch of the Russian Academy of Sciences, 4 Akademicheskoy Ave., 634055 Tomsk, Russia. E-mail: novoselova@ipc.tsc.ru; Tel: +7-3822-491-623*

† Electronic supplementary information (ESI) available: Experimental and characterization details; discussion of process details. See DOI: 10.1039/c7ra09062e



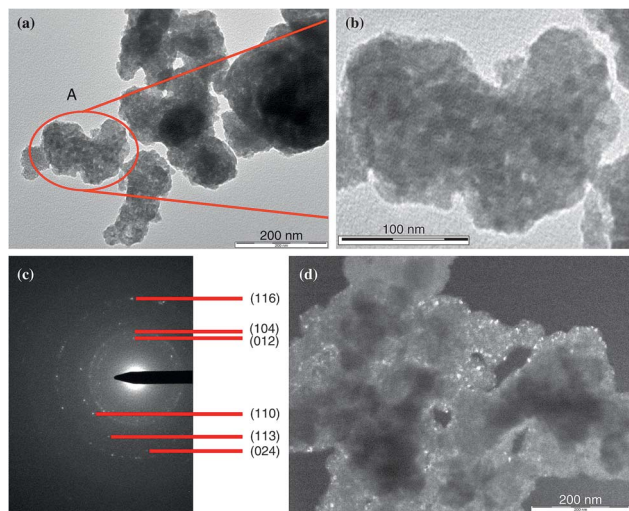


Fig. 1 (a, b, and d) TEM images and (c) electron microdiffraction pattern of HNPCs.

Herein, the synthesis of hematite nanoparticle clusters (HNPCs) with remarkably high magnetization of  $51 \text{ emu g}^{-1}$ , comparable to those of nanoscale magnetite and maghemite, is reported. HNPCs were obtained in a single-step thermal process in which the precursor was treated with the burner without any support (Scheme 1) (for more details, see Section 2.2, ESI†).

The iron ( $\text{Fe}^{3+}$ ) precursor for the synthesis is known as iron removal precipitate (IRP), a waste product obtained from the treatment of natural groundwater for drinking, household, and industrial needs. This waste material is abundant worldwide, especially in regions where groundwater is characterized by an elevated iron content. The FTIR, XRF, XRD, and thermal analysis data collectively show that the IRP starting material is a powder based, primarily, on amorphous iron hydroxides containing a rather large amount of water (Section 3.2, ESI†).

Upon treatment of the IRP with the gas burner flame, a sharp, almost instantaneous evaporation of water takes place, which strips the water out of the material and practically disintegrates the particles of the initial powder at different hierarchical levels. At the same time, oxygen entering the open tube from the air contributes to the synthesis of the most thermodynamically stable form of iron oxide, *i.e.*, hematite. We refer to this procedure as “sharp high-temperature dehydration (SHTDH)”.

The key factor of the SHTDH is the very sharp, short exposure to high temperature of the amorphous iron oxyhydroxide phases (the  $\text{Fe}^{3+}$  ion sources) that contain a considerable amount of adsorbed water in an oxidizing atmosphere. Here, the (i) sharp, high-temperature exposure involves no preheating of the initial material prior to the treatment. The material is exposed to a high temperature immediately. (ii) The short exposure means that there is no maintaining the product at an elevated temperature. Such a holding period could lead to the gradual recrystallization of the synthesized particles, accompanied by an increase in their size and a change in their properties. For more details see Section 4, ESI†.

The described synthesis of HNPCs by SHTDH can be viewed, on the one hand, as a version of the thermal decomposition of

iron precursors. However, it most likely could serve as a starting point for developing a new approach for producing iron oxide-based nanomaterials. It should be noted that this approach agrees well with the principles of “green chemistry,” and, on the other hand, in our opinion, it could be extended to the synthesis of nanomaterials with other compositions.

The results of transmission electron microscopy (TEM) of the powder obtained from the thermal treatment (Fig. 1a–d and S2, ESI†) indicate that hematite nanoparticle clusters were synthesized. These clusters display irregular, somewhat elongated shapes with dimensions of approximately 50–200 nm. Each cluster consists of multiple individual nanoparticles with a mean size of less than 10 nm. Furthermore, the clusters tend to aggregate slightly, rather than remain as isolated entities.<sup>13c,17</sup> This tendency can be explained by the lack of any special techniques to prevent aggregation of the particles in the nanomaterial (*e.g.*, application of various surfactants, polymers, *etc.*) during its preparation. The electron microdiffraction pattern (Fig. 1c), which can be used to clarify atomic crystal structures for phase identification,<sup>18</sup> confirms that hematite was obtained.

The obtained HNPCs were investigated using FTIR spectroscopy. In the region of  $400\text{--}800 \text{ cm}^{-1}$ , two broad transmission bands centered at  $441$  and  $559 \text{ cm}^{-1}$  and two bands as bends (shoulders) at  $480$  and  $631 \text{ cm}^{-1}$  are observed (Fig. 2a). The peaks at  $480$  and  $559 \text{ cm}^{-1}$  can be associated with the perpendicular modes of the Fe–O stretching vibrations in  $\alpha\text{-Fe}_2\text{O}_3$ , and the peaks at  $441$  and  $631 \text{ cm}^{-1}$  can be ascribed to  $\alpha\text{-Fe}_2\text{O}_3$  lattice modes that have polarization parallel to the *c*-axis.<sup>19</sup> Thus, the FTIR spectroscopy data confirm that hematite was prepared in this work. Some broadening of the peaks may have been caused by particle aggregation,<sup>19c</sup> which was noted above in the discussion of the TEM results.

The prepared HNPCs were also characterized by Raman spectroscopy. By this method, iron oxide phases  $\alpha\text{-Fe}_2\text{O}_3$ ,  $\text{Fe}_3\text{O}_4$  and  $\gamma\text{-Fe}_2\text{O}_3$  can be identified nearly unambiguously. The XRD method, for instance, cannot explicitly differentiate between  $\text{Fe}_3\text{O}_4$  and  $\gamma\text{-Fe}_2\text{O}_3$ .<sup>20</sup> To avoid phase changes, which may be induced by the excitation source during collection of the Raman spectra, as previously observed for iron oxides,<sup>21</sup> the spectrum in this study was collected using a low laser power of  $\sim 0.8 \text{ mW}$ .

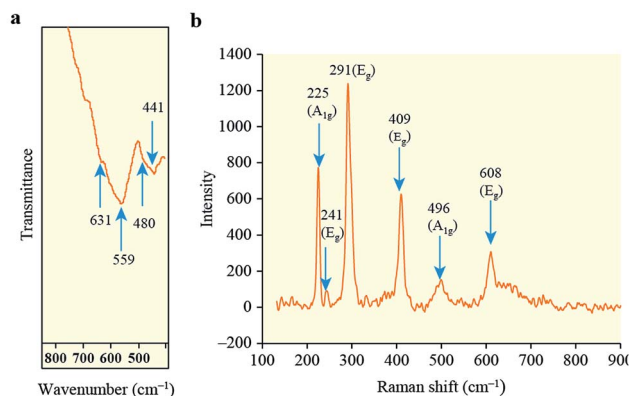


Fig. 2 (a) FTIR and (b) Raman spectra of HNPCs.



At least six lines are clearly visible in the Raman spectrum, at  $\sim 225$ , 241, 291, 409, 496, and  $608\text{ cm}^{-1}$  (Fig. 2b). The peaks at 225 and  $496\text{ cm}^{-1}$  are assigned to the  $A_{1g}$  modes of hematite, and those at 241, 291, 409, and  $608\text{ cm}^{-1}$  are attributed to the  $E_g$  modes of hematite.<sup>21,22</sup> The obtained spectrum thus exhibits six of the seven spectral signatures deemed diagnostic for hematite, and does not contain any peaks associated with either maghemite or magnetite. There is also a shift of the characteristic lines towards lower wavenumbers, which is common for nanoparticles.<sup>22</sup>

Thus, the combined TEM, FTIR, and Raman data clearly demonstrate that hematite nanoparticle clusters were obtained in the present study.

The field dependence of the magnetization of the HNPCs is presented in Fig. 3. The data show an exceptionally high value of saturation magnetization for the HNPCs, reaching  $51\text{ emu g}^{-1}$  at an applied field of  $H = 6.5\text{ kOe}$  and temperature  $T = 300\text{ K}$ . Although this magnetization value is somewhat lower than those obtained for recently synthesized hematite nanoparticles<sup>16c</sup> and nanorods,<sup>16b</sup> it substantially exceeds that of  $\alpha\text{-Fe}_2\text{O}_3$  nanoparticles,  $21\text{ emu g}^{-1}$  ( $H = 10\text{ kOe}$ ,  $T = 300\text{ K}$ )<sup>16a</sup> and, as far as we know, is currently one of the highest of all values obtained for hematite.

Furthermore, the HNPCs magnetization is comparable to or even higher than those of magnetite and maghemite, which are conventionally considered as magnetic iron oxides. For example, for  $\text{Fe}_3\text{O}_4$  nanoparticles prepared at 25, 40, and  $60^\circ\text{C}$ , the saturation magnetization values were 45, 50, and  $50\text{ emu g}^{-1}$ , respectively ( $H = 20\text{ kOe}$ ,  $T = 25^\circ\text{C}$ ).<sup>23</sup> In the case of 42, 30, and  $19\text{ nm}$   $\text{Fe}_3\text{O}_4$  nanoflowers, saturation magnetization values of 33, 45, and  $36\text{ emu g}^{-1}$  were observed, respectively ( $H = 30\text{ kOe}$ ,  $T = 250\text{ K}$ ),<sup>24</sup> whereas, for porous  $\gamma\text{-Fe}_2\text{O}_3$ , this parameter was approximately  $9\text{ emu g}^{-1}$  ( $H = 5\text{ kOe}$ , room temperature).<sup>20b</sup>

The high magnetization value of the HNPCs can be explained by specific effects of the multilevel hierarchical organization of their structure. On the one hand, the presence of the small individual hematite nanoparticles with dimensions of less than  $10\text{ nm}$  can play a major role in this phenomenon; the high magnetization of such nanoparticles can be associated with the contribution of uncompensated surface spins, which tend to interact ferromagnetically.<sup>16a</sup> On the other hand, the clustering

of these individual nanoparticles and the tendency of the resulting clusters to assemble, which we noted when discussing the TEM results, can contribute to the enhancement of magnetization. For example, Ge *et al.*<sup>13c</sup> mentioned that clusters with larger sizes exhibited higher values of magnetization (however, these results describe the behavior of magnetite clusters rather than hematite clusters, as in our case). The interaction of these clusters, in distinction from isolated ones, apparently results in the formation of structures of another hierarchical level (with larger sizes), which increases the value of the magnetization.

Based on these results, new applications of hematite nanomaterials can be anticipated, especially in fields in which a material with both high magnetization and thermodynamic stability is required. The former enables the efficient control of a material's movement in different environments using magnetic fields,<sup>2a,c,d</sup> and, if necessary, separation of the material from those environments.<sup>2b,e,3b</sup> The latter helps the material to maintain the required properties upon exposure to an extended temperature range. Hematite is considered the most thermodynamically stable phase of iron oxide,<sup>14a</sup> in contrast to magnetite and maghemite, which are usually oxidized to  $\alpha\text{-Fe}_2\text{O}_3$  at elevated temperature.<sup>20b,25</sup>

In summary, the hematite nanoparticle clusters with an exceptionally high magnetization of  $51\text{ emu g}^{-1}$ , comparable to the magnetization values of nanoscale magnetite and maghemite, were synthesized for the first time. They were prepared from IRP (a renewable, globally available waste material consisting of iron hydroxides with adsorbed water that is produced during the removal of iron from groundwater). The newly described synthesis has many advantages, including rapidity, environmental friendliness, and single-stage operational simplicity. It does not require modifiers such as templates, catalysts, or surfactants, and avoids the use of toxic and/or expensive reagents or nonrenewable sources of iron. Thus, the synthesis of HNPCs by SHTDH agrees well with the principles of "green chemistry".

It is expected that these HNPCs will find many applications in the development of advanced materials. In addition, the data presented in this paper may (i) lead to a revision of ideas about the magnetic properties of iron oxides, particularly hematite; (ii) suggest the replacement of magnetite and/or maghemite nanomaterials in many applications by hematite nanomaterials as more thermodynamically stable; and (iii) lead to the development of a new approach for the synthesis of nanomaterials.

## Conflicts of interest

There are no conflicts to declare.

## Acknowledgements

The author expresses gratitude to employees of Tomsk Regional Common Use Center for fruitful cooperation. The author is also grateful to the Joint-use Center of Tomsk Scientific Center of SB RAS for providing access to the Nicolet 5700 FTIR spectrometer.

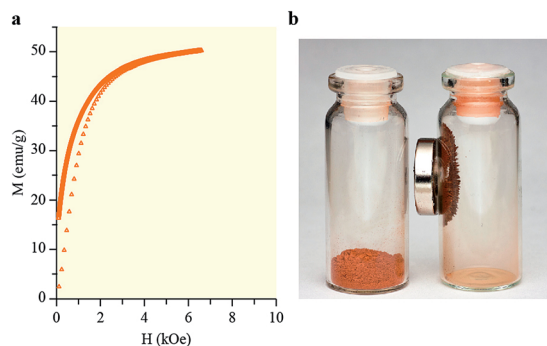


Fig. 3 (a) Dependence of the HNPCs magnetization on the magnetic field. (b) Images of (left) initial IRP material and (right) synthesized HNPCs material with a magnet.





## Notes and references

- 1 (a) L. S. Zhong, J. S. Hu, H. P. Liang, A. M. Cao, W. G. Song and L. J. Wan, *Adv. Mater.*, 2006, **18**, 2426; (b) C. Yang, J. J. Wu and Y. L. Hou, *Chem. Commun.*, 2011, **47**, 5130; (c) T. Peik-See, A. Pandikumar, L. H. Ngee, H. N. Ming and C. C. Hua, *Catal. Sci. Technol.*, 2014, **4**, 4396; (d) S. Lee, A. Fursina, J. T. Mayo, C. T. Yavuz, V. L. Colvin, R. G. S. Sofin, I. V. Shvets and D. Natelson, *Nat. Mater.*, 2008, **7**, 130; (e) S. C. Warren, K. Voitchovsky, H. Dotan, C. M. Leroy, M. Cornuz, F. Stellacci, C. Hebert, A. Rothschild and M. Graetzel, *Nat. Mater.*, 2013, **12**, 842; (f) M. Hu and Y. Yamauchi, *Chem.-Asian J.*, 2011, **6**, 2282.
- 2 (a) Z. Liu, H. S. Wang, C. Liu, Y. J. Jiang, G. Yu, X. D. Mu and X. Y. Wang, *Chem. Commun.*, 2012, **48**, 7350; (b) V. K. Sharma, T. J. McDonald, H. Kim and V. K. Garg, *Adv. Colloid Interface Sci.*, 2015, **225**, 229; (c) P. Calcagnile, D. Fragouli, I. S. Bayer, G. C. Anyfantis, L. Martiradonna, P. D. Cozzoli, R. Cingolani and A. Athanassiou, *ACS Nano*, 2012, **6**, 5413; (d) P. Thanikaivelan, N. T. Narayanan, B. K. Pradhan and P. M. Ajayan, *Sci. Rep.*, 2012, **2**, 230; (e) Q. Zhu, F. Tao and Q. M. Pan, *ACS Appl. Mater. Interfaces*, 2010, **2**, 3141; (f) J. Hu, G. H. Chen and I. M. C. Lo, *Water Res.*, 2005, **39**, 4528; (g) H. Y. Chen, K. L. Lv, Y. Du, H. P. Ye and D. Y. Du, *J. Alloys Compd.*, 2016, **674**, 399; (h) Q. R. Zhang, J. Teng, G. D. Zou, Q. M. Peng, Q. Du, T. F. Jiao and J. Xiang, *Nanoscale*, 2016, **8**, 7085; (i) R. Liu, J. F. Liu, L. Q. Zhang, J. F. Sun and G. B. Jiang, *J. Mater. Chem. A*, 2016, **4**, 7606; (j) V. Chandra, J. Park, Y. Chun, J. W. Lee, I. C. Hwang and K. S. Kim, *ACS Nano*, 2010, **4**, 3979; (k) B. Peng, T. T. Song, T. Wang, L. Y. Chai, W. C. Yang, X. R. Li, C. F. Li and H. Y. Wang, *Chem. Eng. J.*, 2016, **299**, 15; (l) J. T. Mayo, S. S. Lee, C. T. Yavuz, W. W. Yu, A. Prakash, J. C. Falkner and V. L. Colvin, *Nanoscale*, 2011, **3**, 4560; (m) L. Yu. Novoselova, *Powder Technol.*, 2016, **287**, 364; (n) L. Yu. Novoselova, E. E. Sirotkina and N. I. Pogadaeva, *Pet. Chem.*, 2008, **48**, 67; (o) L. Yu. Novoselova and E. E. Sirotkina, *Russ. J. Phys. Chem. A*, 2009, **83**, 2127.
- 3 (a) R. V. Jagadeesh, A. E. Surkus, H. Junge, M. M. Pohl, J. Radnik, J. Rabeah, H. M. Huan, V. Schuenemann, A. Brueckner and M. Beller, *Science*, 2013, **342**, 1073; (b) D. Wang, C. Deraedt, J. Ruiz and D. Astruc, *Acc. Chem. Res.*, 2015, **48**, 1871; (c) C. Bolm, *Nat. Chem.*, 2009, **1**, 420; (d) J. M. Walker and J. M. Zaleski, *Nanoscale*, 2016, **8**, 1535.
- 4 (a) S. Yan and Q. S. Wu, *J. Mater. Chem. A*, 2015, **3**, 5982; (b) Z. Dai, C. S. Lee, Y. Tian, I. D. Kim and J. H. Lee, *J. Mater. Chem. A*, 2015, **3**, 3372; (c) X. L. Hu, J. C. Yu, J. M. Gong, Q. Li and G. S. Li, *Adv. Mater.*, 2007, **19**, 2324; (d) N. D. Cuong, D. Q. Khieu, T. T. Hoa, D. T. Quang, P. H. Viet, T. D. Lam, N. D. Hoa and N. V. Hieu, *Mater. Res. Bull.*, 2015, **68**, 302.
- 5 (a) O. Zandi and T. W. Hamann, *Nat. Chem.*, 2016, **8**, 778; (b) P. Dias, A. Vilanova, T. Lopes, L. Andrade and A. Mendes, *Nano Energy*, 2016, **23**, 70; (c) Z. Sun, E. Madej, A. Genc, M. Muhler, J. Arbiol, W. Schuhmann and E. Ventos, *Chem. Commun.*, 2016, **52**, 7348; (d) Y. Huang, Z. X. Lin, M. B. Zheng, T. H. Wang, J. Z. Yang, F. S. Yuan, X. Y. Lu, L. Liu and D. P. Sun, *J. Power Sources*, 2016, **307**, 649; (e) S. Tanaka, R. R. Salunkhe, Y. V. Kaneti, V. Malgras, S. M. Alshehri, T. Ahamad, M. B. Zakaria, S. X. Dou, Y. Yamauchi and M. S. A. Hossain, *RSC Adv.*, 2017, **7**, 33994.
- 6 (a) K. L. Viola, J. Sbarboro, R. Sureka, M. De, M. A. Bicca, J. Wang, S. Vasavada, S. Satpathy, S. Wu, H. Joshi, P. T. Velasco, K. MacRenaris, E. A. Waters, C. Lu, J. Phan, P. Lacor, P. Prasad, V. P. Dravid and W. L. Klein, *Nat. Nanotechnol.*, 2015, **10**, 91; (b) J. Xie, G. Liu, H. S. Eden, H. Ai and X. Y. Chen, *Acc. Chem. Res.*, 2011, **44**, 883; (c) S. Laurent, D. Forge, M. Port, A. Roch, C. Robic, L. V. Elst and R. N. Muller, *Chem. Rev.*, 2008, **108**, 2064; (d) R. Hachani, M. Lowdell, M. Birchall, A. Hervault, D. Mertz, S. Begin-Coline and T. K. T. Nguyen, *Nanoscale*, 2016, **8**, 3278; (e) H. Arami, A. Khandhar, D. Liggitt and K. M. Krishnan, *Chem. Soc. Rev.*, 2015, **44**, 8576; (f) S. A. Corr, S. J. Byrne, R. Tekoriute, C. J. Meledandri, D. F. Brougham, M. Lynch, C. Kerskens, L. O'Dwyer and Y. K. Gun'ko, *J. Am. Chem. Soc.*, 2008, **130**, 4214.
- 7 (a) H. Hashimoto, M. Nakanishi, H. Asaoka, T. Maeda, Y. Kusano, T. Fujii and J. Takada, *ACS Appl. Mater. Interfaces*, 2014, **6**, 20282; (b) H. Hashimoto, H. Inada, Y. Okazaki, T. Takaishi, T. Fujii and J. Takada, *ACS Appl. Mater. Interfaces*, 2016, **8**, 10918; (c) P. Thanikaivelan, R. Murali and K. Krishnaraj, *RSC Adv.*, 2016, **6**, 6496.
- 8 (a) Y. Ding, L. Zhang, O. L. Liao, G. J. Zhang, S. Liu and Y. Zhang, *Nano Res.*, 2016, **9**, 2018; (b) G. L. Wu, Y. H. Cheng, Y. Y. Ren, Y. Q. Wang, Z. D. Wang and H. J. Wu, *J. Alloys Compd.*, 2015, **652**, 346; (c) H. Zhang, A. J. Xie, C. P. Wang, H. S. Wang, Y. H. Shen and X. Y. Tian, *J. Mater. Chem. A*, 2013, **1**, 8547.
- 9 (a) P. T. Anastas and M. M. Kirchhoff, *Acc. Chem. Res.*, 2002, **35**, 686; (b) P. Anastas and N. Eghbali, *Chem. Soc. Rev.*, 2010, **39**, 301; (c) P. Anastas, B. X. Han, W. Leitner and M. Poliakoff, *Green Chem.*, 2016, **18**, 12.
- 10 (a) T. Hyeon, S. S. Lee, J. Park, Y. Chung and H. Bin Na, *J. Am. Chem. Soc.*, 2001, **123**, 12798; (b) N. R. Jana, Y. F. Chen and X. G. Peng, *Chem. Mater.*, 2004, **16**, 3931; (c) S. P. Gubin, Yu. A. Koksharov, G. B. Khomutov and G. Yu. Yurkov, *Russ. Chem. Rev.*, 2005, **74**, 489; (d) S. T. Aruna and A. S. Mukasyan, *Curr. Opin. Solid State Mater. Sci.*, 2008, **12**, 44; (e) A. Varma, A. S. Mukasyan, A. S. Rogachev and K. V. Manukyan, *Chem. Rev.*, 2016, **116**, 14493; (f) A. I. Gusev and A. A. Rempel, *Nanocrystalline Materials*, Cambridge International Science Publishing, Cambridge, 2004.
- 11 (a) C. T. Yavuz, J. T. Mayo, W. W. Yu, A. Prakash, J. C. Falkner, S. Yean, L. L. Cong, H. J. Shipley, A. Kan, M. Tomson, D. Natelson and V. L. Colvin, *Science*, 2006, **314**, 964; (b) W. W. Yu, J. C. Falkner, C. T. Yavuz and V. L. Colvin, *Chem. Commun.*, 2004, **20**, 2306; (c) A. Demortiere, P. Panissod, B. P. Pichon, G. Pourroy, D. Guillon, B. Donnio and S. Begin-Colin, *Nanoscale*, 2011, **3**, 225.
- 12 (a) F. Ooi, J. S. DuChene, J. J. Qiu, J. O. Graham, M. H. Engelhard, G. X. Cao, Z. Gai and W. D. Wei, *Small*,



- 2015, **11**, 2649; (b) D. Ho, X. L. Sun and S. H. Sun, *Acc. Chem. Res.*, 2011, **44**, 875.
- 13 (a) R. F. Chen, G. Q. Song and Y. Wei, *J. Phys. Chem. C*, 2010, **114**, 13409; (b) S. Zhao and S. Asuha, *Powder Technol.*, 2010, **197**, 295; (c) J. P. Ge, Y. X. Hu, M. Biasini, W. P. Beyermann and Y. D. Yin, *Angew. Chem., Int. Ed.*, 2007, **46**, 4342.
- 14 (a) J. B. Lian, X. C. Duan, J. M. Ma, P. Peng, T. I. Kim and W. J. Zheng, *ACS Nano*, 2009, **3**, 3749; (b) J. M. Ma, J. B. Lian, X. C. Duan, X. D. Liu and W. J. Zheng, *J. Phys. Chem. C*, 2010, **114**, 10671; (c) S. Sivakumar, D. Anusuya, C. P. Khatiwada, J. Sivasubramanian, A. Venkatesan and P. Soundhirarajan, *Spectrochim. Acta, Part A*, 2014, **128**, 69.
- 15 (a) M. Arruebo, R. Fernandez-Pacheco, M. R. Ibarra and J. Santamaria, *Nano Today*, 2007, **2**, 22; (b) A. Dreyer, A. Feld, A. Kornowski, E. D. Yilmaz, H. Noei, A. Meyer, T. Krekeler, C. G. Jiao, A. Stierle, V. Abetz, H. Weller and G. A. Schneider, *Nat. Mater.*, 2016, **15**, 522.
- 16 (a) K. V. Manukyan, Y. S. Chen, S. Rouvimov, P. Li, X. Li, S. N. Dong, X. Y. Liu, J. K. Furduna, A. Orlov, G. H. Bernstein, W. Porod, S. Roslyakov and A. S. Mukasyan, *J. Phys. Chem. C*, 2014, **118**, 16264; (b) H. Karami, J. Ordoukhanian and A. Nezhadali, *Ceram. Int.*, 2015, **41**, 14760; (c) A. Manikandan, J. J. Vijaya and L. J. Kennedy, *J. Nanosci. Nanotechnol.*, 2013, **13**, 2986.
- 17 Y. Deng, D. Qi, C. Deng, X. Zhang and D. Zhao, *J. Am. Chem. Soc.*, 2008, **130**, 28.
- 18 P. B. Hirsch, A. Howie, R. B. Nicholson, D. W. Pashley and M. J. Whelan, *Electron Microscopy of Thin Crystals*, Butterworths, London, 1965.
- 19 (a) L. Lu, L. P. Li, X. J. Wang and G. S. Li, *J. Phys. Chem. B*, 2005, **109**, 17151; (b) S. Hayashi and H. Kanamori, *J. Phys. C: Solid State Phys.*, 1980, **13**, 1529; (c) C. J. Serna, M. Ocana and J. E. Iglesias, *J. Phys. C: Solid State Phys.*, 1987, **20**, 473.
- 20 (a) H. J. Wu, G. L. Wu and L. D. Wang, *Powder Technol.*, 2015, **269**, 443; (b) M. Hu, J. S. Jiang and Y. Zeng, *Chem. Commun.*, 2010, **46**, 1133; (c) M. Hu, A. A. Belik, M. Imura, K. Mibu, Y. Tsujimoto and Y. Yamauchi, *Chem. Mater.*, 2012, **24**, 2698.
- 21 D. L. A. deFaria, S. V. Silva and M. T. deOliveira, *J. Raman Spectrosc.*, 1997, **28**, 873.
- 22 I. V. Chernyshova, M. F. Hochella Jr and A. S. Madden, *Phys. Chem. Chem. Phys.*, 2007, **9**, 1736.
- 23 C. C. Lin, J. M. Ho and M. S. Wu, *Powder Technol.*, 2015, **274**, 441.
- 24 F. Q. Hu, K. W. MacRenaris, E. A. Waters, E. A. Schultz-Sikma, A. L. Eckermann and T. J. Meade, *Chem. Commun.*, 2010, **46**, 73.
- 25 (a) Z. A. Zang, H. B. Yao, Y. X. Zhou, W. T. Yao and S. H. Yu, *Chem. Mater.*, 2008, **20**, 4749; (b) P. C. Wu, W. S. Wang, Y. T. Huang, H. S. Sheu, Y. W. Lo, T. L. Tsai, D. B. Shieh and C. S. Yeh, *Chem.-Eur. J.*, 2007, **13**, 3878.

